

# Sensor Driven Online Coverage Planning for Autonomous Underwater Vehicles\*

Liam Paull<sup>1</sup>, Sajad Saeedi Gharahbolagh<sup>1</sup>, Mae Seto<sup>2</sup>, Howard Li<sup>1</sup>

**Abstract**—At present, autonomous underwater vehicle (AUV) mine countermeasure (MCM) surveys are pre-planned by operators using ladder or zig-zag paths. Such surveys are often conducted with side-looking sonar sensors whose performance is dependant on a number of environment factors, as well as lateral range from the AUV track.

This research presents a sensor driven online approach to seabed coverage for MCM. A method is presented where paths are planned adaptively using a multi-objective optimization. Information theory is combined with a new concept coined branch entropy based on a hexagonal cell decomposition. The result is a planning algorithm that often produces shorter paths than conventional means and is also capable of accounting for environmental factors detected *in situ*. Hardware-in-the-loop simulations and in water trials conducted on the IVER2 AUV show the effectiveness of the proposed method.

## I. INTRODUCTION

Sensor driven path planning refers to a strategy for gathering sensor measurements to support a sensing objective. Various approaches have been proposed for planning the mobile robots' paths with on-board sensors to enable navigation and obstacle avoidance in unstructured dynamic environments. Traditional mission planning methods focus on how sensor measurements best support the robot mission, rather than robot missions that best support the sensing objective. In the case of area coverage for mine countermeasures (MCM), the sensing objective defines the mission.

Autonomous underwater systems technology is lagging behind ground and aerial robotics systems. Underwater robotics is particularly challenging because of the rapid attenuation of high-frequency signals, and the unstructured nature of the environment. These difficulties must be overcome as the U.S. Navy has referred to underwater mine removal as the most problematic mission facing unmanned undersea vehicles and the U.S. Navy at large [1].

In this research, we propose an online approach to autonomously achieve underwater seabed coverage for MCM. Sensor objectives for the coverage task are particularly hard to define because of the uncertainty of sensor measurements, so information gain is exploited as a goodness criterion [2]. However, it is shown that the information gain method alone is not sufficient to achieve global goals when there

is incomplete prior knowledge about the environment. To compensate, the concept of branch entropy is proposed. The approach can be applied to diverse missions and sensors, but is demonstrated on an AUV performing an MCM mission using a side-looking sensor (SLS).

Prior to this work, few if any research proposed online strategies to underwater area coverage. Usually, AUVs mission plans are pre-programmed with waypoints that specify a structured path, such as a zig-zag or lawn mower. In the approach taken here, path planning is achieved through reconciling behaviors that represent the multiple objectives defined for efficient mission completion. The proposed approach has the advantages that:

- 1) The total path and time required to cover a workspace is often shorter,
- 2) There is no need for pre-programmed waypoints,
- 3) The AUV is adaptive to any changes in environmental conditions that can be detected *in situ*,
- 4) The AUV is able to generate paths for complex and non-convex environment shapes such as would typically found in harbors.

The performance of the approach is evaluated via hardware-in-the-loop simulation and implementation on the IVER2 AUV developed by OceanServer Inc.

The remainder of the paper is organized as follows: Section II will provide some background and literature review, Section III describes the proposed solutions, including the information gain and branch entropy behaviors, Section IV discusses the simulation framework, the hardware setup, and shows the results, and Section V makes some general conclusions.

## II. BACKGROUND OF RESEARCH

Path planning for coverage has many important applications, such as floor cleaning, harvesting, mine hunting, lawn mowing, and others. As described in Choset's 2001 survey of complete coverage methods, there are heuristic, random, and cell decomposition techniques [3]. A heuristic defines a set of rules to follow that will result in the entire environment being covered. For example, Acar and Choset's complete coverage algorithm based on sensing critical points [4], and Wein's [5] method of building corridors based on maximizing some quality function. A key facet of these approaches is having obstacles to be able to generate the rules. Cell decomposition is used to divide up the environment into a manageable number of cells or areas that can be searched like a graph or tree. Once all cells have been covered, then the entire workspace has been covered. Decomposition can be

\*This research is supported by Natural Sciences and Engineering Research Council of Canada (NSERC) and Defense R&D Canada - Atlantic.

<sup>1</sup> Liam Paull, Sajad Saeedi Gharahbolagh and Howard Li are members of the Collaboration Based Robotics and Automation (COBRA) Group in the Department of Electrical and Computer Engineering at the University of New Brunswick. {liam.paull, sajad.saeedi.g, howard}@unb.ca

<sup>2</sup> Mae Seto is a member of the Mine and Harbour Defense Group at Defense R&D Canada-Atlantic. Mae.Seto@drdc-rddc.gc.ca.

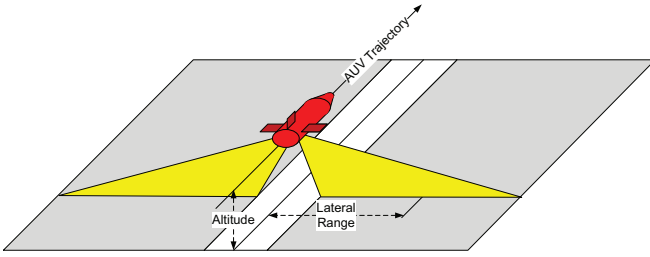


Fig. 1. An example of the AUV trajectory and corresponding area covered by its SSS.

approximate [2], semi-approximate, or exact [3]. The shape of the cells and type of decomposition can have a significant impact on the performance of the search algorithm.

In the underwater applications, [6] presents a coverage algorithm for MCM with an SLS is that uses cell decomposition and exploits the supposed fact that mines are normally placed in lines. In [7], a Boustrophedon decomposition is combined with the generalized Voronoi diagram to derive paths for coverage of a highly unstructured or non-convex environment. However, this algorithm presumes that absolute knowledge of the environment is known *a priori* and all planning is done offline. In [8], a coverage algorithm for MCM with an SLS is proposed that optimizes the spacing between parallel tracks. The metric for optimality is the mean probability of detection of the environment and the dependence of the probability of detection on seabed type and range is described. While the proposed method is very useful, the planned paths are constricted to parallel tracks and planning is done offline. Also closely related to our work, Jakuba and Yoerger use a coverage grid approach for AUVs searching for chemical plumes [9]. Coverage can also be achieved in higher dimensions, for example in [10] an algorithm is developed for sensor coverage of a ship's hull with an AUV.

In our case, seabed is to be scanned with a sidescan sonar sensor (SSS). The SSS uses the returns from emitted high frequency sound to generate an image of the seabed. An object sitting on the seabed will cast a sonar shadow that can be analyzed to determine if the shape is suggestive of a mine. The on-board SSS gathers data as the AUV moves forward in rectilinear motion and leaves a narrow channel of unscanned seabed directly beneath it. An AUV path and corresponding SSS coverage swath are shown in Fig. 1. SSS returns are combined with onboard navigation data to provide georeferenced mosaics of the seabed. The angle of incidence of the sonar beam with the seabed has a significant effect on the resolution of the shadow cast by an object and therefore the probability of successful mine detection and classification. The Extensible Performance and Evaluation Suite for Sonar (ESPRESSO) is a tool developed by the Canadian Navy to evaluate the sonar performance characteristics for a specific set of environmental conditions [11]. The program generates a  $\mathcal{P}(y)$  lateral range curve that indicates the probability that a target at a specified lateral range from a sonar's track will be detected. Parameter values that affect the generation

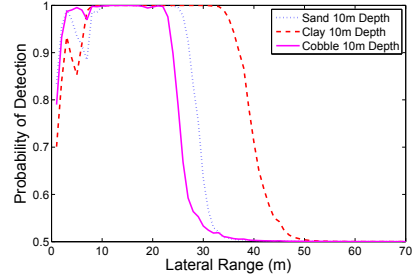


Fig. 2.  $\mathcal{P}(y)$  curves for three different seabed conditions

of the  $\mathcal{P}(y)$  curve include: environmental factors such as seabed type, target properties, sonar attributes, and platform variables such as speed, depth and navigation error. Fig. 2 shows the  $\mathcal{P}(y)$  curves generated by ESPRESSO for three different seabed types: cobble, sand, and clay, all at a depth of 10 m for the Klein 5500 SSS.

### III. PROPOSED METHODS

In the proposed approach, desired headings,  $\psi_d$  are generated by evaluating an objective function over the domain of all possible desired headings:  $\psi = \{0..360\}$ . The general form of the function is given by:

$$\psi_d = \arg \max_{\psi} \{R(\psi)\} \quad (1)$$

$$R(\psi) = w_B B(\psi) + w_G G(\psi) + w_J J(\psi), \quad (2)$$

where  $R$  is the total utility,  $B$  is the information gain,  $G$  is the branch entropy,  $J$  is the benefit of maintaining the current heading, and  $w_B$ ,  $w_G$ , and  $w_J$  are the respective weights.  $B$  prioritizes headings that cover the most area in the short term,  $G$  prioritizes headings that will help the agent complete its coverage mission in the longer term, and  $J(\psi)$  prioritizes headings closest to the current heading so that the AUV will tend to move in straight tracks. The function  $J$  is the simplest and can take the form:

$$J(\psi) \propto -|\psi_c - \psi| + 100 \quad (3)$$

where  $\psi_c$  is the current AUV heading.

The functions  $B$  and  $G$  are generated using the coverage map which is updated as the AUV moves about the workspace. Details will be described in Sections III-A and III-B respectively. Note that optimization takes place over heading only and that it is assumed that desired speed and depth are generated some other way (most likely held constant). It should also be noted that this desired heading is used as a reference to an inner loop controller that produces the desired control plane values. As such, it is reasonable to evaluate (2) over a domain of angles that includes sharp turns. There is no violation of dynamic constraints since these will be imposed in the inner loop. The optimization is evaluated over discretized domains using interval programming (IvP) [12]. In IvP, underlying objective functions are approximated as piecewise linear functions where the accuracy of the representation can be traded off against the

computation time by specifying the number of pieces in the approximation. Tuning of the weights is an important consideration. In the present implementation, trial and error has been used to tune the weights, however, it would be simple to optimize them with some meta heuristic method such as genetic algorithms or particle swarm optimization.

#### A. The Information Gain Behavior

The mutual information  $I$  or expected entropy reduction (EER):

$$I(X, Z) = H(X) - \bar{H}(X|Z), \quad (4)$$

defines a scalar quantity that represents the *a priori* expected information about a state  $X$  contained in an observation  $Z$ .  $H(X) = E[\log P(X)]$  is the Shannon entropy of  $X$  and represents in some way the compactness of the distribution [13]. To evaluate  $\bar{H}(X|Z)$  we take the expectation over the measurement  $Z$ :

$$\begin{aligned} \bar{H}(X|Z) &= E_z\{H(X|Z)\} \\ &= - \int P(Z) \int P(X|Z) \log P(X|Z) dX dZ. \end{aligned} \quad (5)$$

where  $P(Z)$  is the probability of obtaining measurement  $Z$ .

The essential aspect of this definition is that it specifies a way of combining sensor measurements *additively*. Consider some control action at time  $t$  to be  $U(t)$ . If the ratio of the control frequency to the sensor frequency is  $n$  then each control action,  $U(t)$  will result in a set of  $n$  independent measurements  $\{Z_1, Z_2, \dots, Z_n\}$ . The total expected *information gain* of  $U(t)$  can be expressed as:

$$B(U(t)) = \sum_{k=1}^n I(X, Z_k). \quad (6)$$

To define the information gain objective function, information gained must be formulated as a function of heading  $\psi$ . This is achieved by defining a track starting at the AUVs current location,  $(x, y)$ , and traveling a fixed distance,  $r$ , at every potential heading in the domain of the search. The measurements that will be made can be predicted and then (6) can be used to evaluate the expected information gained from traveling along the given track.

Define the variable  $M_{ij} \in \{0, 1\}$  to represent the actual presence or absence of a target at the point  $(i, j)$  in the discretized workspace,  $W$ . Then, consider the variable  $m_{ij} \in \{0, 1\}$  to be our belief about the presence or absence of a mine at location  $(i, j)$ . The confidence at location  $(i, j)$ ,  $c_{ij}$  represents the probability that if a mine exists that it will be detected. Therefore, we can define a binary RV  $T_{ij}$  such that:

$$\begin{aligned} P(T_{ij} = 1) &= P(m_{ij} = M_{ij}) = c_{ij} \\ P(T_{ij} = 0) &= P(m_{ij} \neq M_{ij}) = 1 - c_{ij} \end{aligned} \quad (7)$$

Then the entropy of  $T_{ij}$  can be represented as:

$$H(T_{ij}) = -c_{ij} \log(c_{ij}) - (1 - c_{ij}) \log(1 - c_{ij}) \quad (8)$$

From (8) it follows that

$$\lim_{c_{ij} \rightarrow 1} H(T_{ij}) = 0. \quad (9)$$

This implies that maximizing the confidence over the environment minimizes the entropy of  $T_{ij}$ . From (2), the information gain objective function  $B$  has to be defined as a function of headings  $\psi$ . This function is generated by simulating paths from the AUVs current location in the direction of  $\psi$  and evaluating the expected entropy reduction over the coverage grid variables  $T_{ij}$ . Let the proposed path to be evaluated be represented by  $\mathcal{C}$ . The path begins at the AUV's current location,  $(x, y)$  and moves a distance  $r$  at heading  $\psi$ :

$$\mathcal{C} : [0, 1] \rightarrow C_{free, s} \rightarrow \mathcal{C}(s) \quad (10)$$

$$\mathcal{C}(0) = (x, y) \quad (11)$$

$$\mathcal{C}(1) = (x + r \cos(\psi), y + r \sin(\psi)) \quad (12)$$

Let the proposed action,  $U(t)$  from (5) be defined by the proposed track. Since  $r$ ,  $x$ , and  $y$  are assumed constant, the information gain resulting from following the proposed track can be defined as a function of only the heading,  $\psi$ .

Assume that following this track will result in a series of  $n$  SSS returns that represent measurements  $Z = \{Z_1, Z_2, \dots, Z_n\}$ . Then, (5) can be used to compute the expected entropy at location  $(i, j)$  in the workspace as a result of any individual measurement  $Z_k, k = 1..n$ .

$$\begin{aligned} \bar{H}(T_{ij}|Z_k) &= E_{z_k}\{H(T_{ij}|Z_k)\} \\ &= - \sum_{Z_k} P(Z_k) [-c'_{ij} \log c'_{ij} \\ &\quad - (1 - c'_{ij}) \log (1 - c'_{ij})] \end{aligned} \quad (13)$$

where  $c'_{ij}$  is the posterior confidence at location  $(i, j)$  after measurement  $Z_k$ .

Evaluation of (13) requires knowledge of the distribution of  $Z_k$ . This distribution represents the probability of obtaining the set of environmental conditions that would produce a given  $\mathcal{P}(y)$  lateral range curve. If there is no knowledge of environmental conditions beforehand, this distribution can be initialized as uniform across all environment parameters. As the AUV traverses the workspace, unknown environmental conditions such as seabed type can be determined and the distributions can be updated based on the new knowledge.

The distribution  $P(T_{ij}|Z_k)$  is determined by the appropriate lateral characteristic curve determined using the ESPRESSO model. Sample curves are shown in Fig. 2. The perpendicular distance of point  $(i, j)$  to the path  $\mathcal{C}$  can be found using a simple orthogonal projection, and is the lateral range used to sample the curve. The new confidence obtained from measurement  $Z_k$  should be combined with the existing confidence at  $(i, j)$ ,  $c_{ij}$  to produce the new confidence at that location  $c'_{ij}$  [14].

The EER at location  $(i, j)$  caused by measurement  $Z_k$  then follows from (4) as:

$$I(T_{ij}, Z_k) = H(T_{ij}) - \bar{H}(T_{ij}|Z_k) \quad (14)$$

Define the line that is perpendicular to  $\mathcal{C}$  and aligns with the SSS reading  $Z_k$  as  $\mathcal{C}^\perp$ . The EER over the entire

workspace,  $W$ , brought about by a measurement  $Z_k$  is then the sum of the EER along the line  $C^\perp$ .

$$I(W, Z_k) = \sum_{(i,j) \text{ on } C^\perp} I(T_{ij}, Z_k) \quad (15)$$

Given that there is no overlap between subsequent sonar pings from a SSS, the total expected information gain brought about by moving along the proposed path  $C$  can be expressed as:

$$B(\psi) = \sum_{k=1}^n I(W, Z_k) \quad (16)$$

An AUV is shown in an environment in Fig. 5. The IvP functions at the stop time is shown in Fig. 6. Note that the highest utility for the information gain objective function in this case is approximately  $90^\circ$ , the direction that is being traveled, and the lowest utility is the reverse direction,  $270^\circ$ , because almost no new information would be gained from moving over the path that was just traveled.

### B. Branch Entropy

The information gain method has been shown to be effective for solving the path planning problem when *a priori* knowledge of the environment, obstacles, and targets is available [2]. However, it is common that this information will not be available, or will not be completely accurate. In the sensor-driven approach, the information gain  $B$  is useful for evaluating the benefits over a short horizon, but when complete coverage is the goal, this approach reduces to a greedy-first search (GFS).

It is necessary to include a function  $G$ , termed the branch entropy, in the objective function (2) that helps the AUV achieve its global goal.

To compute the  $G$ , the workspace is first decomposed into  $N$  equally-sized hexagon cells such that the cells cover the entire workspace. The average entropy of the cells are updated as the AUV moves about the environment. On each evaluation of the outer loop controller, each cell  $C_i$  is assigned a level,  $l$ , which is the minimum number of cells that must be traversed to reach that cell from the presently occupied cell  $C_p$ . In addition, each cell maintains a list of children, which are all neighbors in level  $l + 1$ . A directed acyclic graph (DAG) is built using the levels and children of each cell where every cell  $C_i$  appears only once in the graph, and is at level  $l$ . There can be several paths from  $C_p$  to  $C_i$  but they must all be the same minimum length. Each neighbor of  $C_p$  is referred to as a branch and the branch entropy  $G$  quantifies how much uncovered area exists down that particular branch of the DAG.

A hexagon decomposition of a workspace is shown in Fig. 3. The workspace is the shaded area underneath the hexagons. The hexagon on the right shows the numbering convention for the neighbors. The advantage of using a hexagon decomposition is that each cell at level  $l$  is guaranteed to be the same distance from current cell  $C_p$ .

There will be a value of BE for each neighbor of the current cell  $C_p$  as each neighbor has its own branch in the

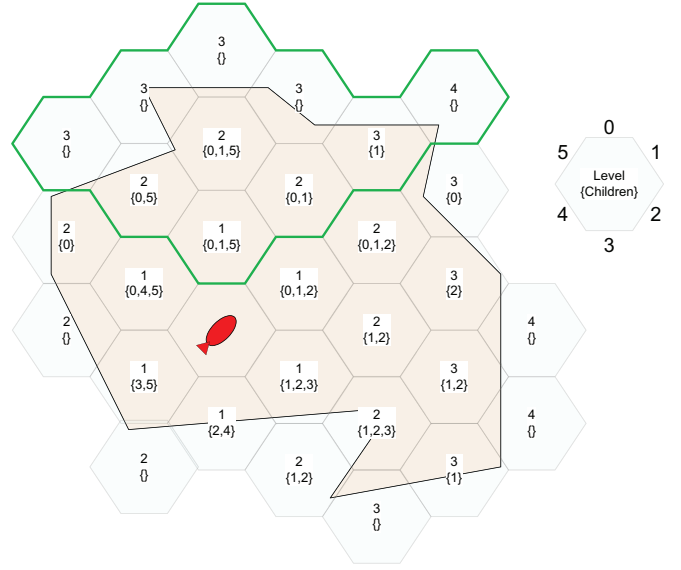


Fig. 3. An environment with a cell decomposition. The cells that will be in branch 0 have been outlined in green.

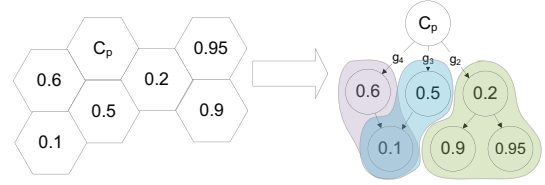


Fig. 4. A transformation from cell to DAG. (numbers in cells/nodes represent average cell entropy)

DAG. For each neighbor,  $k = 0..5$ , of  $C_p$ , the BE,  $g_k$ , for a DAG with a total of  $L$  levels is given by (17).  $m_{lk}$  is the number of nodes in level  $l$  of branch  $k$  and  $\hat{H}_i$  is the average entropy of cell  $C_i$ .

$$g_k = \frac{\sum_{l=2}^L (L-l+1) \frac{\sum_{i=1}^{m_{lk}} \hat{H}_i}{m_{lk}}}{\sum_{l=1}^{L-1} l}. \quad (17)$$

In (17), the closer cells are weighted higher using an inverse linear function so that the AUV will tend to choose branches with uncovered area nearby. Other weighting functions, such as exponential decay could have been used, and would produce similar results.

Fig. 4 shows the transformation from hexagon cells to DAG. The cell labeled  $C_p$  is the cell that the AUV is currently in, and the values in all of the other cells represent their average entropies. The corresponding BE for each of the three neighbors are calculated as:

$$g_4 = 1/3((2)(0.6) + (1)(0.1)) = 0.433,$$

$$g_3 = 1/3((2)(0.5) + (1)(0.1)) = 0.367,$$

$$g_2 = 1/3((2)(0.2) + (1)(1/2)(0.95 + 0.90)) = 0.442.$$

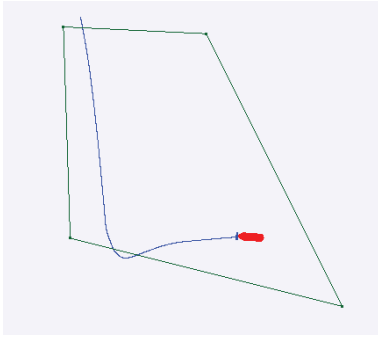


Fig. 5. A simulated path.

In this case  $g_2$  is the highest.

The values of branch entropy are treated as samples of the underlying objective function and are connected linearly to generate the full objective function. The six potential headings of known utility are  $60^\circ \times k, k = 0..5$ , which corresponds to the headings that pass through the midpoints of the neighboring hexagon faces. The corresponding points used to generate the objective function for  $G(\psi)$  are  $(60^\circ \times k, g_k), k = 0..5$ . The known points are then connected with straight lines. A general equation for the objective function,  $G(\psi)$  is derived that parameterizes each of the connecting lines:

$$G(\psi) = \frac{1}{60}(g_k - g_{k+1})\psi + g_k(1 - k) + g_{k+1}, \quad (18)$$

$$k = \lfloor \frac{\psi}{60} \rfloor.$$

Note that for consistency define  $g_6 = g_0$ .

An AUV is shown in an environment in Fig. 5. The IvP functions at the stop time are shown in Fig. 6. The BE behavior is maximum at  $0^\circ$  and  $180^\circ$  as these headings point to the areas of the map that have the largest unfinished areas.

### C. The Collective Objective Function

According to (2), the final utility,  $R$ , is the weighted sum of the objective functions. In Fig. 6 the objective functions at a snapshot are shown together with the collective. In this case, the collective objective function selects the heading at  $94^\circ$  to be the best desired heading.

## IV. RESULTS

In order to test the control algorithms, a Hardware-In-The-Loop (HWIL) simulator was developed using the Mission Oriented Operating Suite (MOOS) [15]. This provided seamless transition to real hardware trials on the Oceanserver Inc. IVER2 (Fig. 7).

### A. Simulation

A Monte Carlo style simulation is conducted to compare the performance for information gain alone, information gain with branch entropy, and a random walk algorithm by repeating the simulation 36 times with random initial conditions. The results are tested against the deterministic typical lawn mower pattern for a simple yet non-convex

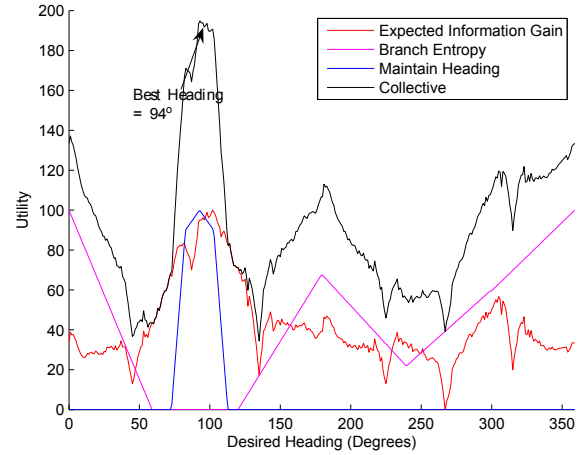


Fig. 6. The information gain, branch entropy, maintain heading, and collective objective functions corresponding to snapshot shown in Fig. 5



Fig. 7. The Iver2 AUV

environment. Results for three different levels of desired confidence are shown in Table I, where values for random, IG and IG/BE are reported as  $\mu[\sigma]$  where  $\mu$  and  $\sigma$  correspond to the mean and the standard deviation of the 36 trials and all values are in meters.

		Desired Confidence		
		.90	.95	.98
Search Method	Lawn Mower	1275	1545	2355
	Random	1279 [446]	1915 [460]	2299 [677]
	IG	1488 [362]	2429 [817]	3307 [730]
	IG/BE	1088 [105]	1458 [150]	1761 [160]

TABLE I

PERFORMANCE OF LAWN MOWER, RANDOM WALK, INFORMATION GAIN AND INFORMATION GAIN WITH BRANCH ENTROPY ALGORITHMS FOR DIFFERENT CONFIDENCE THRESHOLDS.

The simulation results in Table I show that the paths planned by the planner with IG and BE are shorter on average than the paths generated by the lawn mower planner. The authors make no claim that the lawn mower plots tested are necessarily optimal, but they are very reasonable. It should be emphasized the benefits of the proposed online sensor driven planner extend far beyond just the benefits of shorter path lengths, which cannot necessarily be guaranteed. As stated, the proposed planner requires no waypoints and is capable of adapting its mission based on the *actual* coverage obtained. As such, it is guaranteed to converge to complete coverage,

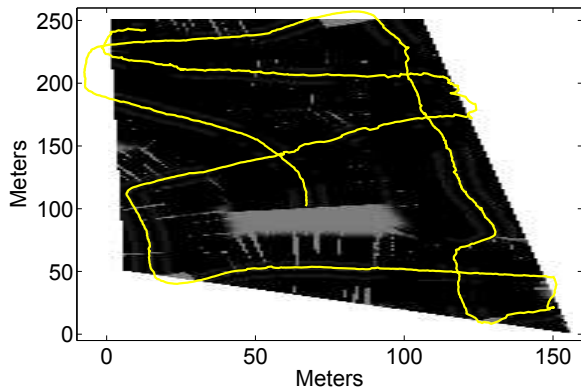


Fig. 8. The path to cover a simple environment with overlaid on top of the resulting confidence. Darker areas indicate higher confidence. The vehicle begins at the top left corner.

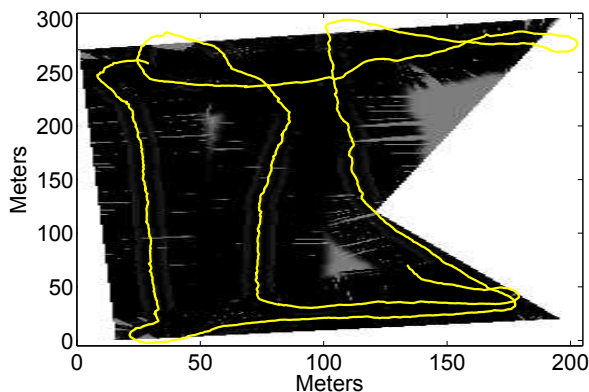


Fig. 9. The path to cover a more complex workspace overlaid on top of the resulting confidence map.

which is not possible for offline planners in reality.

### B. In-Water Trials

The vehicle is equipped with an Inertial Navigation System (INS), a Doppler Velocity Log (DVL), a GPS, and a dual frequency 330/880 Hz Yellowfin sidescan sonar.

The AUV was able to successfully cover two environments within the limited operating region. Plots for two different environments are overlaid on the final confidence maps in Fig. 8 and Fig. 9. The runs were stopped when confidence values reached 95%.

A comparison lawn mower mission was also performed on the environment used for Fig. 8 (path not shown).

The path lengths for each of the three trials are shown in Table II.

## V. CONCLUSION

This research presents an online sensor driven robotics path planner with particular application to seabed coverage with a sidescan sonar sensor on an autonomous underwater vehicle. The approach combines information theory with a new concept coined branch entropy to efficiently cover areas of seabed. Simulation results and real water trials

	Path Length	Workspace Area
Proposed planner (Fig. 8)	1203 m	28 000 $m^2$
Lawn mower	1580 m	
Proposed planner (Fig. 9)	1661 m	41 250 $m^2$

TABLE II

SAMPLE PATH LENGTHS FOR PATHS PLANNED DURING HARDWARE TRIALS

illustrate the benefit of this approach over standard lawn mower planners. These advantages are: the total path length and time to cover an environment are shorter, there is no need for predetermined waypoints, environmental factors can be accounted for, and the planner is able to autonomously handle very complex shaped environments. The method has been tested on a HWIL simulation and on real hardware. The result is an efficient path planner with a higher level of autonomy that standard preprogrammed structured mission plans.

## REFERENCES

- [1] U.S. Navy, "The navy unmanned undersea vehicle (UUV) master plan," Tech rep. a847115, U.S. Navy, 2004.
- [2] Cheghui Cai and Silvia Ferrari, "Information-driven sensor path planning by approximate cell decomposition," *IEEE Transactions on Systems, Man, and Cybernetics - Part B: Cybernetics*, vol. 39, no. 3, pp. 672–689, Jun. 2009.
- [3] Howie Choset, "Coverage for robotics - a survey of recent results," *Annals of Mathematics and Artificial Intelligence*, vol. 31, pp. 113–126, 2001.
- [4] Ercan U. Acar and Howie Choset, "Sensor-based coverage of unknown environments: Incremental construction of morse decompositions," *International Journal of Robotics Research*, vol. 21, pp. 345–367, 2002.
- [5] Ron Wein, Jur van den Berg, and Dan Halperin, "Planning high-quality paths and corridors amidst obstacles," *The International Journal of Robotics Research*, vol. 27, pp. 1213–1231, 2008.
- [6] J.R. Stack and C.M. Smith, "Combining random and data-driven coverage planning for underwater mine detection," in *OCEANS 2003. Proceedings*, Sep. 2003, vol. 5, pp. 2463–2468.
- [7] Cheng Fang and S. Anstee, "Coverage path planning for harbour seabed surveys using an autonomous underwater vehicle," in *OCEANS 2010 IEEE - Sydney*, May 2010, pp. 1–8.
- [8] D.P. Williams, "On optimal AUV track-spacing for underwater mine detection," in *Robotics and Automation (ICRA), 2010 IEEE International Conference on*, May 2010, pp. 4755–4762.
- [9] M. Jakuba and D.R. Yoerger, "Autonomous search for hydrothermal vent fields with occupancy grid maps," in *Proceedings of the Australasian Conference on Robotics and Automation*, 2008.
- [10] B. Englot and F. Hover, "Inspection planning for sensor coverage of 3d marine structures," in *IEEE/RSJ International Conference on Intelligent Robots and Systems (IROS)*, Oct. 2010, pp. 4412–4417.
- [11] G. Davies and E. Signell, "Espresso scientific user guide," Nurc-sp-2006-003, NATO Underwater Research Centre, 2006.
- [12] M.R. Benjamin, J.A. Curcio, and P.M. Newman, "Navigation of unmanned marine vehicles in accordance with the rules of the road," in *Robotics and Automation, 2006. ICRA 2006. Proceedings 2006 IEEE International Conference on*, May 2006, pp. 3581–3587.
- [13] Ben Grocholsky, *Information-Theoretic Control of Multiple Sensor Platforms*, Ph.D. thesis, Australian Centre for Field Robotics, University of Sydney, 2002.
- [14] L. Paull, S. Saeedi, H. Li, and V. Myers, "An information gain based adaptive path planning method for an autonomous underwater vehicle using sidescan sonar," in *IEEE Conference on Automation Science and Engineering (CASE)*, Aug. 2010, pp. 835–840.
- [15] Michael Benjamin, Paul Newman, Henrik Schmidt, and John Leonard, "An overview of MOOS-IvP and a brief users guide to the IvP Helm autonomy software," MIT-CSAIL-TR-2009-028, Jun. 2009.